# EVENTFLASH: TOWARDS EFFICIENT MLLMS FOR EVENT-BASED VISION

**Anonymous authors**
Paper under double-blind review

## ABSTRACT

Event-based multimodal large language models (MLLMs) enable robust perception in high-speed and low-light scenarios, addressing key limitations of frame-based MLLMs. However, current event-based MLLMs often rely on dense image-like processing paradigms, overlooking the spatiotemporal sparsity of event streams and resulting in high computational cost. In this paper, we propose EventFlash, a novel, efficient MLLM to explore spatiotemporal token sparsification for reducing data redundancy and accelerating inference. Technically, we built EventMind, a large-scale and scene-diverse dataset with over 500k instruction sets, providing both short and long event stream sequences to support our curriculum training strategy. Then, we present the adaptive temporal window aggregation module for efficient temporal sampling, which adaptively compresses temporal tokens while retaining key temporal cues. Finally, the sparse density-guided attention module is designed to improve spatial token efficiency by selecting informative regions and suppressing empty or sparse areas. Experimental results show that EventFlash achieves a 12.4$\times$ throughput improvement over the baseline (EventFlash-Zero) while maintaining comparable performance. It supports long-range event stream processing with up to 1,000 bins, significantly outperforming EventGPT's 5-bin limit. We believe EventFlash serves as an efficient foundation model for event-based vision. Our code and dataset details are provided in the supplementary.

## 1 INTRODUCTION

Event cameras (Gallego et al., 2020; Posch et al., 2014; Li & Tian, 2021), bio-inspired vision sensors, operate differently from frame-based cameras. Each pixel responds to intensity changes by generating asynchronous events (Li et al., 2022; Kudithipudi et al., 2025). Due to their high temporal resolution and high dynamic range, event cameras have been applied to various vision tasks (e.g., scene understanding (Zhu et al., 2018; Kong et al., 2024; Yao et al., 2024; Zhou et al., 2024; Li et al., 2025a; Liu et al., 2025; Li et al., 2025b; Zhou & Lee, 2025)) in high-speed or low-light scenarios.

Recent multimodal large language models (MLLMs) (Xiang et al., 2025; Li et al., 2024a; Tang et al., 2025; Huang et al., 2024a; Qian et al., 2024) have achieved remarkable breakthroughs in processing conventional frames and language, showing strong capabilities in scene understanding and visual question answering. However, these models are primarily designed for frame-based inputs and cannot directly handle the unique spatiotemporal properties of event streams. A straightforward approach to extending MLLMs to event-based vision involves converting event streams into dense, image-like representations before feeding them into existing MLLMs (e.g., LLaVA (Liu et al., 2023), GPT-4 (Bubeck et al., 2023), or Qwen (Bai et al., 2023)). However, this transformation often overlooks the inherent spatiotemporal sparsity of event data and introduces substantial redundancy (Gehrig & Scaramuzza, 2024; Messikommer et al., 2020; Wu et al., 2024a). In other words, applying dense image-like processing paradigms to event streams not only incurs significant computational overhead but also substantially limits the effective length and efficiency of event stream understanding. Thus, developing efficient MLLMs that fully exploit the unique spatiotemporal properties of event data remains a critical and unresolved challenge.

Despite recent progress, most existing event-based MLLMs (Liu et al., 2025; Li et al., 2025b; Zhou & Lee, 2025) still rely on dense image-like representations, which hinders computational efficiency and scalability to long event sequences. For example, EventGPT (Liu et al., 2025) converts event streams

into dense token sequences for language modeling. EventVL (Li et al., 2025b) integrates RGB frames with event data to enhance multimodal reasoning. LLaFEA (Zhou & Lee, 2025) employs frame-event fusion for region-level spatiotemporal grounding. Although these models perform well in challenging scenarios such as high-speed motion and low-light conditions, their dense processing of sparse event data leads to significant overhead and limits real-time or long-range understanding. Meanwhile, the scene diversity of their datasets is relatively limited, and the event streams are short, making it difficult to support general-purpose models for long event-stream understanding.

In this paper, we propose EventFlash, a novel efficient MLLM that leverages spatiotemporal token sparsification to reduce data redundancy and accelerate inference. Unlike prior works that focus on maximizing reasoning accuracy, our goal is to address three key challenges in efficient MLLMs: (i) *Temporal inefficiency*: The microsecond resolution of event streams results in prohibitively large token volumes when processed over long temporal durations; (ii) *Spatial inefficiency*: The inherent sparsity of event data leads to numerous empty or low-information tokens that incur computational overhead due to uniform attention allocation; (iii) *Dataset limitations*: Existing instruction-augmented datasets are not publicly available and often lack diversity, contain low-quality annotations, and cover short temporal sequences, making them inadequate for training generalizable models.

To address these challenges, our EventFlash presents a density-aware spatiotemporal token sparsification strategy that exploits the inherent sparsity and high temporal resolution of event streams. Specifically, we propose an adaptive temporal window aggregation module for efficient temporal sampling, which dynamically compresses temporal tokens while preserving essential temporal cues. Then, a sparse density-guided attention module is presented to enhance spatial token efficiency by selecting informative regions and suppressing empty or low-density areas. Moreover, we design a progressive curriculum learning strategy following a short-to-long paradigm to improve EventFlash's generalization and generative capabilities. To support this, we built a large-scale scene-diverse dataset over 500k instruction sets, including both short and long event stream sequences. Experimental results show that EventFlash achieves a 12.4× improvement in throughput over our baseline (EventFlash-Zero) while maintaining comparable performance. Notably, EventFlash enables long-range event stream processing of up to 1,000 bins compared to only 5 bins in the competing EventGPT.

In summary, the main contributions of this work are:

- We propose EventFlash, ***an efficient event-based vision MLLM***, which explores a spatiotemporal token sparsification strategy for raw event streams to reduce redundancy, accelerate inference (12.4× throughput), and enable long-range event stream understanding (up to 1,000 bins).
- We present a *density-aware spatiotemporal token sparsification* strategy for event-based MLLMs, which effectively reduces redundancy while maintaining comparable reasoning accuracy by leveraging the fine-grained temporal resolution and inherent sparsity of raw event streams.
- We build a *large-scale scene-diverse dataset for long-range event stream understanding*. We believe this standardized dataset will accelerate future research in event-based MLLMs.

## 2 Related Work

**Event-based Vision with MLLMs.** Early works (Wu et al., 2023; Zhou et al., 2023) have explored the alignment between event data and textual information. Event-CLIP (Wu et al., 2023) builds on pre-trained vision-language models (Radford et al., 2021; Yang et al., 2023; Klenk et al., 2024; Huang et al., 2024b) for event-based recognition, and EventBind (Zhou et al., 2023) incorporates an event encoder to unify images, events, and texts. Yet both overlook the world knowledge embedded in LLMs, constraining nuanced scene understanding. More recently, emerging event-based MLLMs (Liu et al., 2025; Li et al., 2025b; Zhou & Lee, 2025) have demonstrated strong reasoning capabilities in challenging conditions. For example, EventGPT (Liu et al., 2025) is the first to design an event-based MLLM for accurate description and generation. EventVL (Li et al., 2025b) enhances robustness by fusing complementary modalities from event streams and RGB frames. LLaFEA (Zhou & Lee, 2025) achieves region-level spatiotemporal grounding through the complementary fusion of frame and event modalities. However, these event-based LLMs rely on dense image-like processing of inherently sparse events (Peng et al., 2024; Perot et al., 2020; Vemprala et al., 2021; Zhu et al., 2022; Tulyakov et al., 2019; Qu et al., 2024; Lin et al., 2023; Shrestha & Orchard, 2018; Wu et al., 2024b; Engelken, 2023; Cho et al., 2024; Wan et al., 2022; Mei et al., 2023), leading to excessive computation and hindering long-sequence inference.

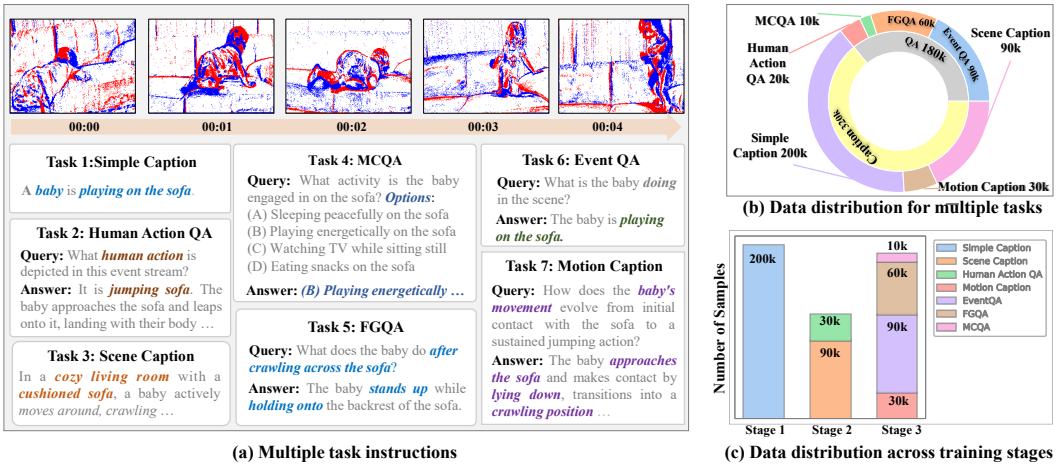


Figure 1: Instructions and data statistics of our EventMind. (a) Seven tasks instructions for event stream understanding. (b) Data distributions of each task. (c) Data distributions of the three stages.

**Efficient Token Sparsification in MLLMs.** Recent MLLMs (Weng et al., 2024; Jiang et al., 2025; Qian et al., 2024) have revealed that visual tokens extracted from foundation models like CLIP contain substantial redundancy, leading to significant computational overhead. Consequently, several token sparsification strategies (Yehezkel et al., 2024; He et al., 2024; Zhang et al., 2024) have been attempted to reduce token counts while preserving essential semantics in video tasks. *However, asynchronous events differ fundamentally from structured frames: while video redundancy mainly stems from spatial repetition within a regular patch grid, event streams consist of sparse spatiotemporal points with redundancy arising from uneven temporal sampling. Their tokens are distributed irregularly and vary in density, making frame-based sparsification not only computationally costly but also ineffective for long event stream understanding.* Thus, this work presents a novel spatiotemporal token sparsification strategy specifically tailored for event streams.

## 3 EventMind Dataset

**Data Collection**. To support the curriculum learning strategy in our EventFlash, we construct a large-scale multimodal dataset named EventMind for event stream understanding. EventMind provides long temporal sequences, diverse scenes, multiple tasks, and high-quality instructions. The raw event data is sourced from both real-world and synthetic domains. Real-world data includes short-duration event sequences from DSEC (Gehrig et al., 2021) and N-ImageNet (Kim et al., 2021), as well as longer-duration streams from HARDVS (Wang et al., 2024b) and E2VID (Rebecq et al., 2019). Synthetic data are generated by converting large-scale video datasets (i.e., Kinetics-700 (Carreira et al., 2019), UCF-101 (Soomro et al., 2012), Wevid-10 M (Bain et al., 2021), PLM-Data (Cho et al., 2025), and MotionBench (Hong et al., 2025)) into event streams using the V2E simulator (Hu et al., 2021). To ensure high-quality simulated events, we use GPT-4o to automatically filter videos using their captions before simulation. To align with our curriculum stages, we categorize them into three groups: short (0–50 ms), medium (50–5,000 ms), and long (5,000–20,000 ms).

**Instruction Generation**. To evaluate the modeling capacity and generalization ability of our EventFlash, we define seven distinct task types for event stream understanding. As shown in Fig. 1(a), these tasks include motion captioning, event question answering (Event QA), human action QA, multiple-choice QA (MCQA), simple captioning, fine-grained QA (FGQA), and scene captioning. Text instructions are constructed via two pathways: (i) For samples with existing textual annotations, we use GPT-4o to refine the descriptions by removing static attributes and irrelevant visual details (e.g., texture, color), ensuring better alignment with event streams. (ii) For samples lacking ground-truth text, we leverage Qwen-VL-Max to automatically generate annotations from corresponding video inputs, enabling a scalable and consistent data synthesis pipeline. In addition, we organize a multi-person team to manually inspect and filter the generated instruction sets for quality assurance.

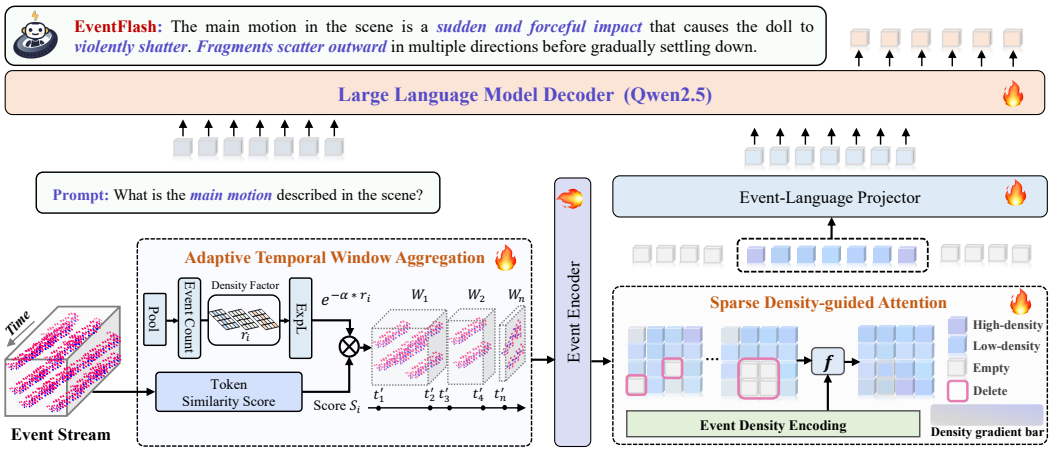


Figure 2: The pipeline of efficient MLLMs (**EventFlash**). The adaptive temporal window aggregation module is presented for efficient temporal sampling, which adaptively compresses temporal tokens while retaining key temporal cues. Besides, the sparse density-guided attention module is designed to improve spatial token by selecting informative regions and suppressing empty or sparse areas.

**Dataset Statistics**. We analyze the composition of the EventMind dataset from a curriculum learning perspective (see Fig. 1(b)). It is structured into three stages based on event sequence length and task complexity. In Stage 1, short sequences are used for the simple captioning task, contributing 200k instruction samples. Stage 2 utilizes medium-length sequences for scene captioning and human action understanding, with a total of 110k instructions. Stage 3 focuses on long sequences for more complex tasks such as motion captioning, EventQA, FGQA, and MCQA, comprising 190k instructions. Overall, our EventMind comprises 500k instruction samples spanning seven task types (see Fig. 1(c)): 200k for simple captioning, 90k for scene captioning, 30k for motion captioning, 90k for EventQA, 60k for FGQA, 10k for MCQA, and 20k for human action QA.

All in all, the novel event-text modality and labor-intensive design make EventMind a highly competitive dataset with several key strengths: (i) *High temporal sampling resolution at the microsecond level from event streams*; (ii) *Coverage of temporal sequences of various lengths*; (iii) *Diverse scene types supporting 7 distinct tasks*; (iv) *A large-scale high-quality instruction set with 500k samples*.

# 4 METHOD

## 4.1 EVENTFLASH OVERVIEW

This work aims at designing an efficient MLLM for event stream understanding, termed EventFlash, which presents a spatiotemporal token sparsification strategy to reduce redundancy and accelerate inference. As illustrated in Fig. 2, our framework consists of five modules: ***adaptive temporal window aggregation module***, ***sparse density-guided attention module***, event encoder, event-language projector, and large language model (LLM) decoder. More precisely, the adaptive temporal window aggregation module first segments the continuous event stream into uniform short bins and adaptively merges adjacent bins based on token similarity or event density. These processed bins are then passed by an event encoder (e.g., CLIP) to extract semantic embeddings. In parallel, the sparse density-guided attention module improves spatial token efficiency by emphasizing informative regions and suppressing empty or low-density areas. The event-language projector aligns the event tokens with text tokens to enable coherent multimodal fusion. Finally, the compact event tokens are fused with text tokens and processed by an LLM decoder (e.g., Qwen-2.5) for multimodal generation tasks.

## 4.2 TEMPORAL SPARSE

The microsecond-level resolution of raw event streams generates an excessive number of temporal tokens, resulting in high computational overhead. To address this, we introduce a two-stage density-guided adaptive temporal window aggregation (ATWA) module that compresses event streams while

preserving key motion dynamics. The event stream is first divided into fine-grained bins, which are iteratively merged based on an asynchronous spatiotemporal spike metric (Li et al., 2022). Each bin is treated as a polarity-aware spatiotemporal point process with an intensity function $\lambda_B$:

$$\lambda_B(x, y, t, p) = \sum_{e_n \in B} f(p_n) \cdot \exp\left(-\frac{(x - x_n)^2}{2\sigma_x^2} - \frac{(y - y_n)^2}{2\sigma_y^2} - \frac{(t - t_n)^2}{2\sigma_t^2}\right), \tag{1}$$

where $f(p_n)$ encodes the polarity for an event $(x_n, y_n, t_n, p_n)$. $\sigma_x$, $\sigma_y$, and $\sigma_z$ are the parameters of the Gaussian kernel. The similarity distance between two bins $B_i$ and $B_{i+1}$ can be computed as:

$$D(B_i, B_{i+1}) = \left\| \lambda_{B_i} - \lambda_{B_{i+1}} \right\|_2, \tag{2}$$

where a lower $D$ indicates higher temporal correlation between two bins. We iteratively merge adjacent bins when the distance is below a threshold $\tau$, forming meta event windows $\{M_1, M_2, \ldots, M_K\}$.

In the second stage, we perform semantic-aware aggregation of meta bins. Each window $M_i$ is passed through an event encoder (e.g., ViT (Arnab et al., 2021)) to obtain a CLS token representation $z_i$, and the similarity $S_i$ between adjacent windows is defined as cosine similarity as follows:

$$S_i = \frac{z_i^\top z_{i+1}}{\|z_i\| \cdot \|z_{i+1}\|}. \tag{3}$$

To incorporate event sparsity, we define a normalized event density factor $r_i = \frac{1}{|M_i|} \sum_{e_n \in M_i} \mathbf{1}_{e_n}$, and compute a density-aware weight. The final adaptive merging score can be formulated by:

$$A_i = S_i \cdot \exp(-\alpha \cdot r_i), \tag{4}$$

where $\alpha$ controls the decay sensitivity. which jointly considers semantic similarity and event sparsity. We iteratively merge windows with high $A_i$ to obtain a compressed yet semantically meaningful temporal sequence that preserves key temporal cues with reduced computational cost.

### 4.3 Spatial Sparse

While temporal aggregation reduces sequence length, spatial redundancy still persists due to the inherent sparsity and uneven event distribution across the sensor plane. To tackle this, we propose the sparse density-guided attention (SDGA) module (see Fig. 3), which adaptively prunes uninformative tokens based on both visual semantics and event density. For each aggregated event bin, we use an encoder (i.e., ViT) to extract patch-level features $\{x_j\}_{j=1}^n$, which are fed into a multi-head self-attention mechanism as:

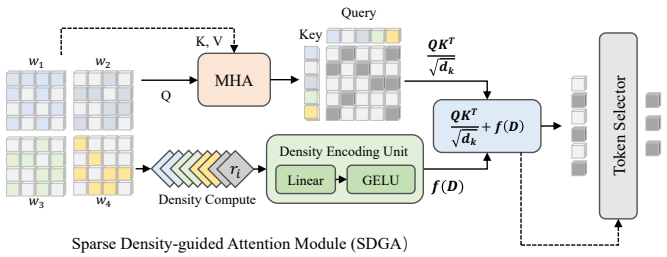


Figure 3: The architecture of the sparse density-guided attention module. It enhances spatial token efficiency by selecting informative regions and suppressing empty or low-density areas.

$$\text{Attention}(Q, K, V) = \text{softmax}\left(\frac{QK^\top}{\sqrt{d_k}}\right) V, \tag{5}$$

where $Q$, $K$, and $V$ are the projected queries, keys, and values from $\{x_j\}$, and $d_k$ is the key dimension.

In parallel, we compute the event density $D_j$ of each token region based on the number of events falling within its receptive field. This scalar value is then passed through a density encoding unit consisting of a linear transformation followed by GELU activation:

$$f(D_j) = \text{GELU}(\text{Linear}(D_j)), \tag{6}$$

where $f(D_j)$ is a soft modulation signal that reflects the importance of each spatial token. The encoded density is added to the attention scores to focus on denser and more important areas as:

$$\tilde{A}_{ij} = \frac{Q_i K_j^\top}{\sqrt{d_k}} + f(D_j). \tag{7}$$

Finally, we apply a *Token Selector* operation that ranks the aggregated attention responses and discards low-importance tokens, which can be formulated as follows:

$$\hat{x}_i = \text{TokenSelector}\left(\sum_j \text{softmax}(\tilde{A}_{ij}) \cdot V_j\right). \tag{8}$$

In summary, this density-guided token pruning strategy enables EventFlash to keep important spatial details while greatly cutting down on redundant computations. By combining semantic relevance with event density, SDGA produces more compact tokens for the efficient MLLM.

### 4.4 Short-to-Long Curriculum Learning

To support scalable training across different event durations and enhance generalization, we propose a progressive short-to-long curriculum learning strategy. Unlike prior event-based MLLMs such as EventVL (Li et al., 2025b) and EventGPT (Liu et al., 2025), which train different modules in separate stages, our curriculum emphasizes a gradual progression from short to long event streams. This design facilitates smoother training dynamics, enabling EventFlash to evolve from mastering simple alignments to handling complex reasoning and long-range event understanding.

To be specific, ***Stage 1*** focuses on event-language alignment by training on 200k short sequences (0-50 ms) paired with simple scene descriptions to establish basic cross-modal understanding. ***Stage 2*** expands to 110k medium sequences (50-5,000 ms) featuring complex motions like human actions, enhancing the model's reasoning and ability to handle instruction-following and event-based QA over longer inputs. ***Stage 3*** fine-tunes the model on 190k long sequences (5,000–20,000 ms) with rich scene descriptions, enabling holistic scene understanding and open-ended language generation.

## 5 Experiments

### 5.1 Experimental Setup

**Implements Details.** We initialize the event encoder with CLIP-ViT-Large-Patch14 (Radford et al., 2021) and use Qwen2.5 (Bai et al., 2023) as the LLM backbone. A two-layer MLP serves as the Event-Language Projector to align the event and semantic spaces. EventFlash is implemented in both 3B and 7B variants and trained on 8 A100 GPUs. For throughput evaluation, the inference is conducted on an A100 GPU using Hugging Face deployment. Our three-stage curriculum learning strategy proceeds as follows: only the Event-Language alignment module is trained in Stage 1, using a learning rate of $2 \times 10^{-3}$ and a batch size of 64. For Stage 2 and Stage 3, all model parameters are unfrozen and trained with a learning rate of $2 \times 10^{-5}$, a batch size of 8, and a gradient accumulation step of 4. A cosine learning rate decay schedule is applied throughout training. We set the temporal aggregation interval to 10 ms and use a density attenuation factor $\alpha$ of 0.1 for spatial sparsification.

**Evaluation Metrics.** To thoroughly evaluate the generalization and reasoning capabilities of our EventFlash, we adopt four metrics aligned with protocols established in LLaVA (Liu et al., 2023) and other widely used benchmarks (Fang et al., 2024). More precisely, we use the following evaluation metrics: (i) Global detailed captioning (GDC) to assess scene-level summarization, (ii) Fine-grained question answering (FGQA) to evaluate the model's understanding of localized event details, (iii) Human action question answering (HAQA) to measure temporal reasoning at the action level, and (iv) Multiple choice question answering (MCQA) to assess instruction-following and discriminative reasoning. For open-ended tasks (GDC and FGQA), we employ LLM-based evaluation using GPT-4o (i.e., LLM-Judge) consistent with prior benchmarks. For HAQA and MCQA, we report the accuracy based on exact matches with ground-truth answers. In addition, throughput and maximum event bin capacity are used to evaluate the efficiency of all MLLMs. Throughput is typically defined as the number of tokens generated per second during inference, while maximum event bin capacity refers to the largest number of event bins the model can process in a single input.

### 5.2 Qualitative results

**Comparison with State-of-the-Art MLLMs.** To evaluate the effectiveness and efficiency of EventFlash, we compare it against four state-of-the-art video-based MLLMs and the only open-

Table 1: Comparison of video-based MLLMs and event-based MLLMs on our EventMind dataset and EventChat-Sub dataset (Liu et al., 2025). Notably, it can process significantly longer event bins than the event-based competitor EventGPT.

| Models | Params | LLM Backbone | Max Bins | Throughput (Token/s) | EventMind | | | | EventChat-Sub | |
|---|---|---|---|---|---|---|---|---|---|---|
| | | | | | GDC | FGQA | HAQA | MCQA | GDC | FGQA |
| **Video-Base ~3B Scale MLLMs** | | | | | | | | | | |
| **Qwen2.5 VL** (Bai et al., 2023) | 3B | Qwen2.5 | 768 | – | 20.6 | 41.7 | 23.8 | 34.6 | 34.5 | 51.2 |
| **VideoChat2-Flash** (Li et al., 2024b) | 2B | Qwen2.5 | 1,000 | – | 31.6 | 38.9 | 16.2 | 43.6 | 36.9 | 43.8 |
| **InternVL2.5** (Lu et al., 2025) | 4B | Qwen2.5 | – | – | 17.9 | 37.0 | 21.3 | 27.3 | 28.9 | 44.6 |
| **Video-Base ~7B Scale MLLMs** | | | | | | | | | | |
| **VideoChat2-Flash** (Li et al., 2024b) | 7B | Qwen2.5 | 1,000 | – | 36.2 | 41.9 | 18.9 | 48.2 | 53.1 | 53.6 |
| **LLaVA-Next-Video** (Liu et al., 2023) | 7B | Qwen2.5 | 56 | – | 31.2 | 44.6 | 22.8 | 42.7 | 46.3 | 54.8 |
| **Qwen2.5 VL** (Bai et al., 2023) | 7B | Qwen2.5 | 768 | – | 22.1 | 43.9 | 28.6 | 41.8 | 41.6 | 53.2 |
| **InternVL2.5** (Lu et al., 2025) | 8B | InternLM2.5 | – | – | 19.7 | 40.0 | 25.3 | 38.2 | 42.5 | 55.6 |
| **Event-Base MLLMs** | | | | | | | | | | |
| **EventGPT-7B** (Liu et al., 2025) | 7B | Vicuna-v1.5 | 5 | 42.2 | – | – | – | – | 71.2 | 78.2 |
| **EventFlash-Zero** | 3B | Qwen-2.5 | **1,000** | 2.3 | 45.3 | 60.4 | 85.0 | 58.2 | 70.4 | 77.1 |
| **EventFlash-3B (Ours*)** | 3B | Qwen-2.5 | **1,000** | 28.5 | 46.8 | 61.1 | 84.9 | 60.0 | 71.5 | 78.6 |
| **EventFlash-7B (Ours*)** | 7B | Qwen-2.5 | **1,000** | 24.0 | **52.3** | **64.2** | **87.6** | **63.1** | **74.1** | **79.5** |

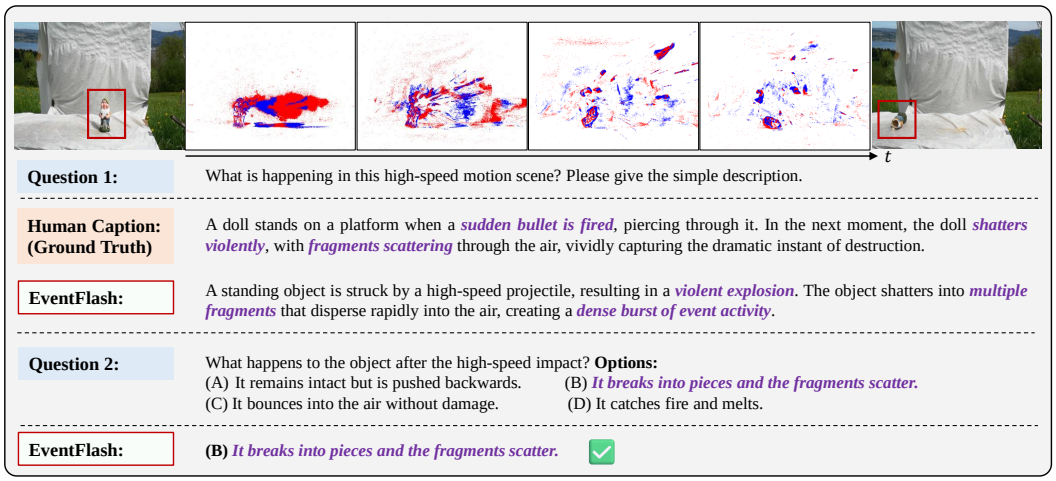


Figure 4: Representative visualization tests on motion captioning and multiple-choice question answering (MCQA) are conducted in high-speed scenarios. Our EventFlash demonstrates superior accuracy in recognizing fast-moving objects, such as a sudden bullet being fired at a doll.

sourced event-based MLLM (i.e., EventGPT (Liu et al., 2025)). We select strong video-based models at both the 3B and 7B scales, including Qwen2.5-VL (Bai et al., 2023), VideoChat2-Flash (Li et al., 2024b), LLaVA-Next-Video (Liu et al., 2023), and InternVL 2.5 (Lu et al., 2025). EventGPT uses fixed bin encoding for event stream understanding. We also construct a baseline, EventFlash-Zero, by removing spatiotemporal sparsification from EventFlash.

**Qualitative Evaluation.** As illustrated in Table 1, EventFlash outperforms four video-based MLLMs and the event-based EventGPT on all four tasks (i.e., GDC, FGQA, HAQA, and MCQA). This demonstrates that EventFlash excels at understanding and describing dynamic event scenes. While EventGPT implements a fixed configuration of 5 event bins, EventFlash can process up to 1,000 event bins, achieving a 200× increase in processing capacity. In other words, our EventFlash is enabled by our efficient sparsification strategy for longer-term understanding. In addition, EventFlash reaches a speed of 28.5 tokens per second during inference. This is 12.4× faster than our baseline EventFlash-Zero (2.3 tokens per second), and it still maintains comparable performance on all tasks.

**Visualization Evaluation.** We further evaluate EventFlash under challenging scenarios, such as high-speed motion and low illumination. As shown in Fig. 4 and Fig. 5, our model demonstrates strong descriptive and reasoning capabilities in both cases. *In high-speed case:* The scene depicts a goblin being struck by a high-velocity projectile, resulting in a mid-air explosion with scattered fragments.

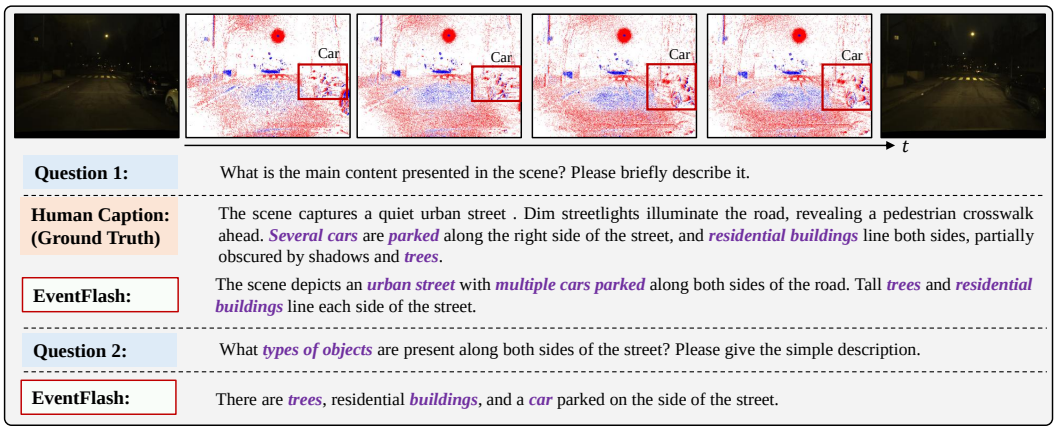


Figure 5: Representative visualization tests on event questioning answering (QA) and scene caption are conducted in low-light scenarios. EventFlash showcases strong scene description and reasoning capabilities, such as identifying a car in a nighttime scene where it is barely visible on RGB images.

EventFlash generates an accurate and fine-grained description of this dynamic event and correctly answers a multiple-choice question. *In low-light case:* The scenario involves a vehicle driving through darkness. Despite the absence of frame-based visual cues, EventFlash generates a coherent and precise description, along with an accurate response to the corresponding QA prompt. These results validate EventFlash's ability to understand complex dynamics in edge-case environments where traditional frame-based models often fail.

To further demonstrate the advantages of EventFlash on long-duration event streams, we compare it with EventGPT on a 10,000 ms sequence. As shown in Fig. 6, EventGPT operates on a fixed number of bins (e.g., 0–50 ms), limiting its understanding to moment-level segments. In contrast, EventFlash leverages its high maximum event bin capacity to process extended sequences, enabling coherent reasoning across the full temporal window and capturing sequence-level motion dynamics. As a result, EventFlash generates more contextually accurate descriptions, highlighting its potential for real-world applications that require long-range understanding, such as surveillance analysis and autonomous driving. More experimental details are in the Appendix.

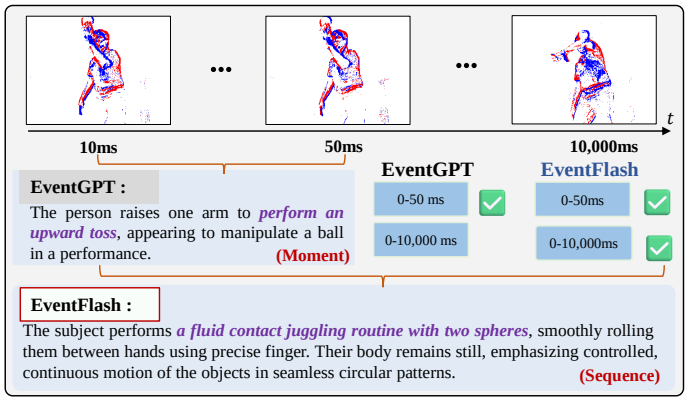


Figure 6: Comparison of EventFlash and EventGPT on long-duration event streams from our EventMind dataset.

## 5.3 Ablation Study

**Contribution of Each Component**. To explore the impact of each component on overall performance, we conduct an ablation study by comparing our full model against three variants: a baseline without any sparsification (EventFlash-Zero), a model with only temporal sparsification, and a model with only spatial sparsification. As shown in Table 2, our full model

Table 2: The contribution of each component to our EventMind dataset. The baseline uses our EventFlash without the spatiotemporal token sparsification strategy.

| Model | S | T | Token/s | EventMind | | | |
|---|---|---|---|---|---|---|---|
| | | | | GDC | FGQA | HAQA | MCQA |
| Baseline | ✗ | ✗ | 2.3 | 45.3 | 60.4 | 85.0 | 58.2 |
| A | ✓ | ✗ | $5.3_{+2.3\times}$ | 46.3 | 61.2 | 85.1 | 59.6 |
| B | ✗ | ✓ | $14.0_{+6.1\times}$ | 47.1 | 60.6 | 83.8 | 60.3 |
| **Ours*** | ✓ | ✓ | $28.5_{+12.4\times}$ | 46.8 | 61.1 | 84.9 | 60.0 |

achieves a 12.4× increase in throughput (28.5 tokens/s vs. 2.3 tokens/s) while maintaining comparable performance across four evaluation metrics (i.e., GDC, FGQA, HAQA, and MCQA). With temporal sparsification alone, the model achieves 14.0 tokens/s, representing a 6.1× speedup over the baseline. In contrast, spatial sparsification alone yields a 2.3× improvement, reaching 5.3 tokens/s. The results show that both temporal and spatial sparsification contribute to efficiency gains.

**Influence of the Aggregation Interval Length**. To explore how the initial temporal bin duration affects performance and efficiency, we evaluate model throughput and accuracy across different initial event bin durations. As shown in Table 3, we compare four settings with bin lengths of 5 ms, 10 ms, 20 ms, and 30 ms. We observe that shorter bin durations (e.g., 5 ms) provide finer temporal resolution but significantly increase the number of windows, resulting in lower throughput (15.8 tokens/s) compared to our default setting of 28.5 tokens/s at 10 ms. Despite the increased computational load, the model maintains strong performance across all tasks. Conversely, increasing the bin size to 20 ms and 30 ms improves throughput to 52.6 and 63.3 tokens/s, respectively, indicating greater efficiency. However, this comes at the cost of performance degradation on GDC, FGQA, MCQA, and HAQA. In this work, a bin duration of 10 ms offers a trade-off between accuracy and efficiency, and is therefore adopted as our default setting.

Table 3: The influence of aggregation interval length on our EventMind dataset.

| Aggregation interval | Throughput (Token/s) | EventMind | | | |
|---|---|---|---|---|---|
| | | GDC | FGQA | MCQA | HAQA |
| 5ms | 15.8 | 47.1 | **61.8** | 84.6 | 58.2 |
| 10ms | 28.5 | **46.8** | 61.1 | **84.9** | **60.0** |
| 20ms | 52.6 | 43.2 | 56.3 | 72.6 | 48.4 |
| 30ms | 63.3 | 36.8 | 48.2 | 61.8 | 46.2 |

**Impact of Density Attenuation Factor $\alpha$.** We investigate how the density attenuation factor $\alpha$ affects model throughput and task performance (see Table 4). To explore the trade-off between density-guided and similarity-guided token merging, we evaluate four values of $\alpha$ to identify the optimal balance between accuracy and efficiency. The results show that increasing $\alpha$ leads to higher throughput, indicating that stronger density suppression accelerates the token aggregation process. For example, FGQA and MCQA stay mostly stable when $\alpha$ is between 0.2 and 0.4. However, GDC and HAQA rely more on detailed timing information. Because of this, their performance drops when $\alpha$ gets higher. The results confirm the effectiveness of our density-aware weighting mechanism. Notably, $\alpha = 0.1$ and $\alpha = 0.4$ achieve a favorable trade-off, providing substantial speed gains while preserving strong task performance.

Table 4: The influence of density factor $\alpha$ on throughput and performance on our EventMind dataset.

| Density Factor $\alpha$ | Throughput (Token/s) | GDC | FGQA | MCQA | HAQA |
|---|---|---|---|---|---|
| 0.1 | 28.5 | 46.8 | 61.1 | 84.9 | 60.0 |
| 0.2 | 27.6 | 45.6 | 61.4 | 85.2 | 58.4 |
| 0.4 | 28.8 | 45.3 | 61.6 | 85.2 | 58.4 |
| 0.6 | 26.8 | 47.2 | 60.8 | 83.2 | 60.1 |

### 5.4 Extensive Application

We further investigate additional downstream applications enabled by our EventFlash. For instance, EventFlash can be readily fine-tuned to support action recognition tasks. As shown in 5, we evaluate its performance on the DailyDVS-200 (Wang et al., 2024a) dataset, where EventFlash predicts action categories in an open-ended QA setting. Our EventFlash achieves outstanding performance and strong generalization capability.

Table 5: Action recognition results on processed DailyDVS-200 (Wang et al., 2024a) dataset.

| Methods | Venue | Input Type | Backbone | top-1 acc. (%) |
|---|---|---|---|---|
| **Swin-T** (Liu et al., 2022) | CVPR'22 | Frame | Transformer | 48.06 |
| **GET** (Peng et al., 2023) | ICCV'23 | Event | Transformer | 37.28 |
| **SDT** (Yao et al., 2023) | NeurIPS'24 | Event | Transformer | 35.43 |
| **ESTF** (Wang et al., 2024b) | AAAI'24 | Event | ResNet50 | 24.68 |
| **EventFlash** | Ours* | Event | Qwen2.5 | **48.36** |

## 6 Conclusion

This paper presents EventFlash, a novel efficient MLLM that leverages spatiotemporal token sparsification to reduce data redundancy and accelerate inference. We also built a large-scale dataset for event stream understanding. The results show that EventFlash achieves a 12.4× improvement in throughput over our baseline (EventFlash-Zero) while maintaining comparable performance. Notably, EventFlash enables long-range event stream processing of up to 1,000 bins compared to only 5 bins in the EventGPT. Our EventFlash serves as an efficient foundational model for event-based vision.

## REFERENCES


Anurag Arnab, Mostafa Dehghani, Georg Heigold, Chen Sun, Mario Lučić, and Cordelia Schmid. Vivit: A video vision transformer. In *Proceedings of the IEEE/CVF International Conference on Computer Vision*, pp. 6836–6846, 2021.

Jinze Bai, Shuai Bai, Yunfei Chu, Zeyu Cui, Kai Dang, Xiaodong Deng, Yang Fan, Wenbin Ge, Yu Han, Fei Huang, et al. Qwen technical report. *arXiv*, 2023.

Max Bain, Arsha Nagrani, Gül Varol, and Andrew Zisserman. Frozen in time: A joint video and image encoder for end-to-end retrieval. In *Proceedings of the IEEE/CVF International Conference on Computer Vision*, pp. 1728–1738, 2021.

Sébastien Bubeck, Varun Chadrasekaran, Ronen Eldan, Johannes Gehrke, Eric Horvitz, Ece Kamar, Peter Lee, Yin Tat Lee, Yuanzhi Li, Scott Lundberg, et al. Sparks of artificial general intelligence: Early experiments with gpt-4. *arXiv*, 2023.

Joao Carreira, Eric Noland, Chloe Hillier, and Andrew Zisserman. A short note on the kinetics-700 human action dataset. *arXiv*, 2019.

Hoonhee Cho, Taewoo Kim, Yuhwan Jeong, and Kuk-Jin Yoon. A benchmark dataset for event-guided human pose estimation and tracking in extreme conditions. *Proceedings of the Advances in Neural Information Processing Systems*, 37:134826–134840, 2024.

Jang Hyun Cho, Andrea Madotto, Effrosyni Mavroudi, Triantafyllos Afouras, Tushar Nagarajan, Muhammad Maaz, Yale Song, Tengyu Ma, Shuming Hu, Suyog Jain, et al. Perceptionlm: Open-access data and models for detailed visual understanding. *arXiv*, 2025.

Rainer Engelken. Sparseprop: Efficient event-based simulation and training of sparse recurrent spiking neural networks. *Proceedings of the Advances in Neural Information Processing Systems*, 36:3638–3657, 2023.

Xinyu Fang, Kangrui Mao, Haodong Duan, Xiangyu Zhao, Yining Li, Dahua Lin, and Kai Chen. Mmbench-video: A long-form multi-shot benchmark for holistic video understanding. *Proceedings of the Advances in Neural Information Processing Systems*, 37:89098–89124, 2024.

Guillermo Gallego, Tobi Delbrück, Garrick Orchard, Chiara Bartolozzi, Brian Taba, Andrea Censi, Stefan Leutenegger, Andrew J Davison, Jörg Conradt, Kostas Daniilidis, et al. Event-based vision: A survey. *IEEE Transactions on Pattern Analysis and Machine Intelligence*, 44(1):154–180, 2020.

Daniel Gehrig and Davide Scaramuzza. Low-latency automotive vision with event cameras. *Nature*, 629(8014):1034–1040, 2024.

Mathias Gehrig, Willem Aarents, Daniel Gehrig, and Davide Scaramuzza. Dsec: A stereo event camera dataset for driving scenarios. *IEEE Robotics and Automation Letters*, 6(3):4947–4954, 2021.

Yefei He, Feng Chen, Jing Liu, Wenqi Shao, Hong Zhou, Kaipeng Zhang, and Bohan Zhuang. Zipvl: Efficient large vision-language models with dynamic token sparsification and kv cache compression. *arXiv*, 2024.

Wenyi Hong, Yean Cheng, Zhuoyi Yang, Weihan Wang, Lefan Wang, Xiaotao Gu, Shiyu Huang, Yuxiao Dong, and Jie Tang. Motionbench: Benchmarking and improving fine-grained video motion understanding for vision language models. *arXiv*, 2025.

Yuhuang Hu, Shih-Chii Liu, and Tobi Delbruck. v2e: From video frames to realistic dvs events. In *Proceedings of the IEEE/CVF Conference on Computer Vision and Pattern Recognition*, pp. 1312–1321, 2021.

Bin Huang, Xin Wang, Hong Chen, Zihan Song, and Wenwu Zhu. Vtimellm: Empower llm to grasp video moments. In *Proceedings of the IEEE/CVF Conference on Computer Vision and Pattern Recognition*, pp. 14271–14280, 2024a.

Zhenpeng Huang, Chao Li, Hao Chen, Yongjian Deng, Yifeng Geng, and Limin Wang. Data-efficient event camera pre-training via disentangled masked modeling. *arXiv*, 2024b.

Jindong Jiang, Xiuyu Li, Zhijian Liu, Muyang Li, Guo Chen, Zhiqi Li, De-An Huang, Guilin Liu, Zhiding Yu, Kurt Keutzer, et al. Token-efficient long video understanding for multimodal llms. *arXiv*, 2025.

Junho Kim, Jaehyeok Bae, Gangin Park, Dongsu Zhang, and Young Min Kim. N-imagenet: Towards robust, fine-grained object recognition with event cameras. In *Proceedings of the IEEE/CVF International Conference on Computer Vision*, pp. 2146–2156, 2021.

Simon Klenk, David Bonello, Lukas Koestler, Nikita Araslanov, and Daniel Cremers. Masked event modeling: Self-supervised pretraining for event cameras. In *Proceedings of the IEEE/CVF Winter Conference on Applications of Computer Vision*, pp. 2378–2388, 2024.

Lingdong Kong, Youquan Liu, Lai Xing Ng, Benoit R Cottereau, and Wei Tsang Ooi. Openess: Event-based semantic scene understanding with open vocabularies. In *Proceedings of the IEEE/CVF Conference on Computer Vision and Pattern Recognition*, pp. 15686–15698, 2024.

Dhireesha Kudithipudi, Catherine Schuman, Craig M Vineyard, Tej Pandit, Cory Merkel, Rajkumar Kubendran, James B Aimone, Garrick Orchard, Christian Mayr, Ryad Benosman, et al. Neuromorphic computing at scale. *Nature*, 637(8047):801–812, 2025.

Bohao Li, Yuying Ge, Yixiao Ge, Guangzhi Wang, Rui Wang, Ruimao Zhang, and Ying Shan. Seed-bench: Benchmarking multimodal large language models. In *Proceedings of the IEEE/CVF Conference on Computer Vision and Pattern Recognition*, pp. 13299–13308, 2024a.

Jianing Li and Yonghong Tian. Recent advances in neuromorphic vision sensors: A survey. *Chinese Journal of Computers*, 44(6):1258–1286, 2021.

Jianing Li, Jia Li, Lin Zhu, Xijie Xiang, Tiejun Huang, and Yonghong Tian. Asynchronous spatio-temporal memory network for continuous event-based object detection. *IEEE Transactions on Image Processing*, 31:2975–2987, 2022.

Ke Li, Gengyu Lyu, Hao Chen, Bochen Xie, Zhen Yang, Youfu Li, and Yongjian Deng. Know where you are from: Event-based segmentation via spatio-temporal propagation. In *Proceedings of the AAAI Conference on Artificial Intelligence*, volume 39, pp. 4806–4814, 2025a.

Pengteng Li, Yunfan Lu, Pinghao Song, Wuyang Li, Huizai Yao, and Hui Xiong. Eventvl: Understand event streams via multimodal large language model. *arXiv*, 2025b.

Xinhao Li, Yi Wang, Jiashuo Yu, Xiangyu Zeng, Yuhan Zhu, Haian Huang, Jianfei Gao, Kunchang Li, Yinan He, Chenting Wang, et al. Videochat-flash: Hierarchical compression for long-context video modeling. *arXiv*, 2024b.

Xiuhong Lin, Changjie Qiu, Siqi Shen, Yu Zang, Weiquan Liu, Xuesheng Bian, Matthias Müller, Cheng Wang, et al. E2pnet: Event to point cloud registration with spatio-temporal representation learning. *Proceedings of the Advances in Neural Information Processing Systems*, 36:18076–18089, 2023.

Haotian Liu, Chunyuan Li, Qingyang Wu, and Yong Jae Lee. Visual instruction tuning. *Proceedings of the Advances in Neural Information Processing Systems*, 36:34892–34916, 2023.

Shaoyu Liu, Jianing Li, Guanghui Zhao, Yunjian Zhang, Xin Meng, Fei Richard Yu, Xiangyang Ji, and Ming Li. Eventgpt: Event stream understanding with multimodal large language models. In *Proceedings of the IEEE/CVF Conference on Computer Vision and Pattern Recognition*, 2025.

Ze Liu, Jia Ning, Yue Cao, Yixuan Wei, Zheng Zhang, Stephen Lin, and Han Hu. Video swin transformer. In *Proceedings of the IEEE/CVF conference on computer vision and pattern recognition*, pp. 3202–3211, 2022.

Dongchen Lu, Yuyao Sun, Zilu Zhang, Leping Huang, Jianliang Zeng, Mao Shu, and Huo Cao. Internvl-x: Advancing and accelerating internvl series with efficient visual token compression. *arXiv*, 2025.

Haiyang Mei, Zuowen Wang, Xin Yang, Xiaopeng Wei, and Tobi Delbruck. Deep polarization reconstruction with pdavis events. In *Proceedings of the IEEE/CVF Conference on Computer Vision and Pattern Recognition*, pp. 22149–22158, 2023.

Nico Messikommer, Daniel Gehrig, Antonio Loquercio, and Davide Scaramuzza. Event-based asynchronous sparse convolutional networks. In *Proceedings of the European Conference on Computer Vision*, pp. 415–431, 2020.

Yansong Peng, Yueyi Zhang, Zhiwei Xiong, Xiaoyan Sun, and Feng Wu. Get: Group event transformer for event-based vision. in 2023 ieee. In *CVF International Conference on Computer Vision (ICCV)*, volume 1, pp. 4, 2023.

Yansong Peng, Hebei Li, Yueyi Zhang, Xiaoyan Sun, and Feng Wu. Scene adaptive sparse transformer for event-based object detection. In *Proceedings of the IEEE/CVF Conference on Computer Vision and Pattern Recognition*, pp. 16794–16804, 2024.

Etienne Perot, Pierre De Tournemire, Davide Nitti, Jonathan Masci, and Amos Sironi. Learning to detect objects with a 1 megapixel event camera. *Proceedings of the Advances in Neural Information Processing Systems*, 33:16639–16652, 2020.

Christoph Posch, Teresa Serrano-Gotarredona, Bernabe Linares-Barranco, and Tobi Delbruck. Retinomorphic event-based vision sensors: bioinspired cameras with spiking output. *Proceedings of the IEEE*, 102(10):1470–1484, 2014.

Rui Qian, Xiaoyi Dong, Pan Zhang, Yuhang Zang, Shuangrui Ding, Dahua Lin, and Jiaqi Wang. Streaming long video understanding with large language models. *Proceedings of the Advances in Neural Information Processing Systems*, 37:119336–119360, 2024.

Qiang Qu, Xiaoming Chen, Yuk Ying Chung, and Yiran Shen. Evrepsl: Event-stream representation via self-supervised learning for event-based vision. *IEEE Transactions on Image Processing*, 2024.

Alec Radford, Jong Wook Kim, Chris Hallacy, Aditya Ramesh, Gabriel Goh, Sandhini Agarwal, Girish Sastry, Amanda Askell, Pamela Mishkin, Jack Clark, et al. Learning transferable visual models from natural language supervision. In *Proceedings of the International Conference on Machine Learning*, pp. 8748–8763. PmLR, 2021.

Henri Rebecq, René Ranftl, Vladlen Koltun, and Davide Scaramuzza. Events-to-video: Bringing modern computer vision to event cameras. In *Proceedings of the IEEE/CVF Conference on Computer Vision and Pattern Recognition*, pp. 3857–3866, 2019.

Sumit B Shrestha and Garrick Orchard. Slayer: Spike layer error reassignment in time. *Proceedings of the Advances in neural information processing systems*, 31, 2018.

Khurram Soomro, Amir Roshan Zamir, and Mubarak Shah. Ucf101: A dataset of 101 human actions classes from videos in the wild. *arXiv*, 2012.

Yunlong Tang, Jing Bi, Siting Xu, Luchuan Song, Susan Liang, Teng Wang, Daoan Zhang, Jie An, Jingyang Lin, Rongyi Zhu, et al. Video understanding with large language models: A survey. *IEEE Transactions on Circuits and Systems for Video Technology*, 2025.

Stepan Tulyakov, Francois Fleuret, Martin Kiefel, Peter Gehler, and Michael Hirsch. Learning an event sequence embedding for dense event-based deep stereo. In *Proceedings of the IEEE/CVF International Conference on Computer Vision*, pp. 1527–1537, 2019.

Sai Vemprala, Sami Mian, and Ashish Kapoor. Representation learning for event-based visuomotor policies. *Proceedings of the Advances in Neural Information Processing Systems*, 34:4712–4724, 2021.

Zhexiong Wan, Yuchao Dai, and Yuxin Mao. Learning dense and continuous optical flow from an event camera. *IEEE Transactions on Image Processing*, 31:7237–7251, 2022.

Qi Wang, Zhou Xu, Yuming Lin, Jingtao Ye, Hongsheng Li, Guangming Zhu, Syed Afaq Ali Shah, Mohammed Bennamoun, and Liang Zhang. Dailydvs-200: A comprehensive benchmark dataset for event-based action recognition. In *European Conference on Computer Vision*, pp. 55–72. Springer, 2024a.

Xiao Wang, Zongzhen Wu, Bo Jiang, Zhimin Bao, Lin Zhu, Guoqi Li, Yaowei Wang, and Yonghong Tian. Hardvs: Revisiting human activity recognition with dynamic vision sensors. In *Proceedings of the AAAI Conference on Artificial Intelligence*, volume 38, pp. 5615–5623, 2024b.

Yuetian Weng, Mingfei Han, Haoyu He, Xiaojun Chang, and Bohan Zhuang. Longvlm: Efficient long video understanding via large language models. In *Proceedings of the European Conference on Computer Vision*, pp. 453–470. Springer, 2024.

Sheng Wu, Hang Sheng, Hui Feng, and Bo Hu. Egsst: Event-based graph spatiotemporal sensitive transformer for object detection. *Proceedings of the Advances in Neural Information Processing Systems*, 37:120526–120548, 2024a.

Song Wu, Zhiyu Zhu, Junhui Hou, Guangming Shi, and Jinjian Wu. E-motion: Future motion simulation via event sequence diffusion. *Proceedings of the Advances in Neural Information Processing Systems*, 37:105552–105582, 2024b.

Ziyi Wu, Xudong Liu, and Igor Gilitschenski. Eventclip: Adapting clip for event-based object recognition. *arXiv*, 2023.

Jinxi Xiang, Xiyue Wang, Xiaoming Zhang, Yinghua Xi, Feyisope Eweje, Yijiang Chen, Yuchen Li, Colin Bergstrom, Matthew Gopaulchan, Ted Kim, et al. A vision–language foundation model for precision oncology. *Nature*, pp. 1–10, 2025.

Yan Yang, Liyuan Pan, and Liu Liu. Event camera data pre-training. In *Proceedings of the IEEE/CVF International Conference on Computer Vision*, pp. 10699–10709, 2023.

Bowen Yao, Yongjian Deng, Yuhan Liu, Hao Chen, Youfu Li, and Zhen Yang. Sam-event-adapter: Adapting segment anything model for event-rgb semantic segmentation. In *Proceedings of the IEEE International Conference on Robotics and Automation*, pp. 9093–9100. IEEE, 2024.

Man Yao, Jiakui Hu, Zhaokun Zhou, Li Yuan, Yonghong Tian, Bo Xu, and Guoqi Li. Spike-driven transformer. *Advances in neural information processing systems*, 36:64043–64058, 2023.

Oryan Yehezkel, Alon Zolfi, Amit Baras, Yuval Elovici, and Asaf Shabtai. Desparsify: Adversarial attack against token sparsification mechanisms. *Proceedings of the Advances in Neural Information Processing Systems*, 37:127536–127560, 2024.

Yuan Zhang, Chun-Kai Fan, Junpeng Ma, Wenzhao Zheng, Tao Huang, Kuan Cheng, Denis Gudovskiy, Tomoyuki Okuno, Yohei Nakata, Kurt Keutzer, et al. Sparsevlm: Visual token sparsification for efficient vision-language model inference. *arXiv*, 2024.

Hanyu Zhou and Gim Hee Lee. Llafea: Frame-event complementary fusion for fine-grained spatiotemporal understanding in lmms. *arXiv*, 2025.

Jiazhou Zhou, Xu Zheng, Yuanhuiyi Lyu, and Lin Wang. E-clip: Towards label-efficient event-based open-world understanding by clip. *arXiv*, 2023.

Jiazhou Zhou, Xu Zheng, Yuanhuiyi Lyu, and Lin Wang. Eventbind: Learning a unified representation to bind them all for event-based open-world understanding. In *European Conference on Computer Vision*, pp. 477–494, 2024.

Alex Zihao Zhu, Dinesh Thakur, Tolga Özaslan, Bernd Pfrommer, Vijay Kumar, and Kostas Daniilidis. The multivehicle stereo event camera dataset: An event camera dataset for 3d perception. *IEEE Robotics and Automation Letters*, 3(3):2032–2039, 2018.

Zhiyu Zhu, Junhui Hou, and Xianqiang Lyu. Learning graph-embedded key-event back-tracing for object tracking in event clouds. *Proceedings of the Advances in Neural Information Processing Systems*, 35:7462–7476, 2022.

# EVENTFLASH: TOWARDS EFFICIENT MLLMS FOR EVENT-BASED VISION – SUPPLEMENTARY MATERIAL–

## A EVENT CAMERA SENSING MECHANISM

Event cameras, namely dynamic vision sensors (DVS), asynchronously detect pixel-wise intensity changes instead of recording absolute luminance, emulating the operation of biological retinas. Unlike conventional frame-based cameras that capture images at fixed intervals, DVS generate sparse event streams, significantly improving computational efficiency. Each event $e_n$ occurs asynchronously when the logarithmic brightness variation at the pixel $\mathbf{u}_n = (x_n, y_n)$ surpasses a preset threshold $C$:

$$\log\left(\frac{I(x_n, y_n, t_n)}{I(x_n, y_n, t_n - \Delta t)}\right) = p_n C, \tag{9}$$

where $p_n \in \{+1, -1\}$ indicates the polarity of brightness change, and $\Delta t$ denotes the time elapsed since the previous event at the same pixel. Consequently, the event stream can be described as:

$$\mathcal{E} = \{e_n\}_{n=1}^{N} = \{(x_n, y_n, t_n, p_n)\}_{n=1}^{N}, \tag{10}$$

The inherent sparsity and asynchronous generation of event data facilitate ultra-low latency, enabling robust performance under high-speed motion and low-light conditions. Furthermore, event cameras possess an exceptional dynamic range exceeding 120 dB, significantly surpassing conventional imaging sensors. However, directly applying dense image-like processing paradigms to event streams overlooks their high temporal resolution and sparsity, two of their most critical advantages, resulting in substantial spatiotemporal redundancy. In this work, we aim at designing a spatiotemporal token sparsification strategy tailored for efficient and expressive event stream understanding.

## B MULTI-STAGE TRAINING PIPELINE

**Stage 1: Event-Language Alignment.** This stage establishes a foundational alignment between event representations and textual semantics. We train the model using 200k short-duration (0-50 ms) event streams paired with simple yet descriptive scene captions. By focusing on fine-grained, low-level event-language associations, this stage effectively facilitates initial cross-modal grounding while mitigating interference from complex, long-range temporal dependencies.

**Stage 2: Temporal Reasoning Tuning.** To enhance spatiotemporal reasoning, we extend training to 200k medium-length event sequences ranging from 50 ms to 5,000 ms. These samples include complex motion patterns such as human action recognition, which require the model to capture fine-grained dynamics and temporal dependencies. This stage strengthens the model's capacity for instruction following and event-based question answering over temporally extended inputs.

**Stage 3: Long-Term Scene Understanding.** In the final stage, we fine-tune the model on 100k long-duration (5,000–20,000 ms) event streams paired with diverse high-quality language annotations. This enhances the model's ability to understand complex temporal dynamics and generate coherent outputs in long-range scenarios.

## C MORE DATASET DETAILS

We construct **EventMind**, a large-scale and temporally diverse event-text dataset tailored for long-range event stream understanding. The dataset comprises over 500k high-quality samples spanning 7 tasks with varying temporal lengths, and is designed to support evaluation under four key metrics. Our EventMind enables comprehensive training and benchmarking of event-based multimodal large language models

Table 6: Summary of our EventMind dataset.

| Task | Data Source | Scale |
|---|---|---|
| Simple Caption | DSEC, N-ImageNet | 200k |
| Human Action QA | Kinetics-700, UCF-101, HARDVS | 30k |
| Scene Caption | Wevid-10M, PLM-Data | 90k |
| MCQA | PLM-Data | 10k |
| FGQA | E2VID, PLM-Data, Wevid-10M | 60k |
| EventQA | Wevid-10M, Kinetics | 90k |
| Motion Caption | MotionBench | 30k |

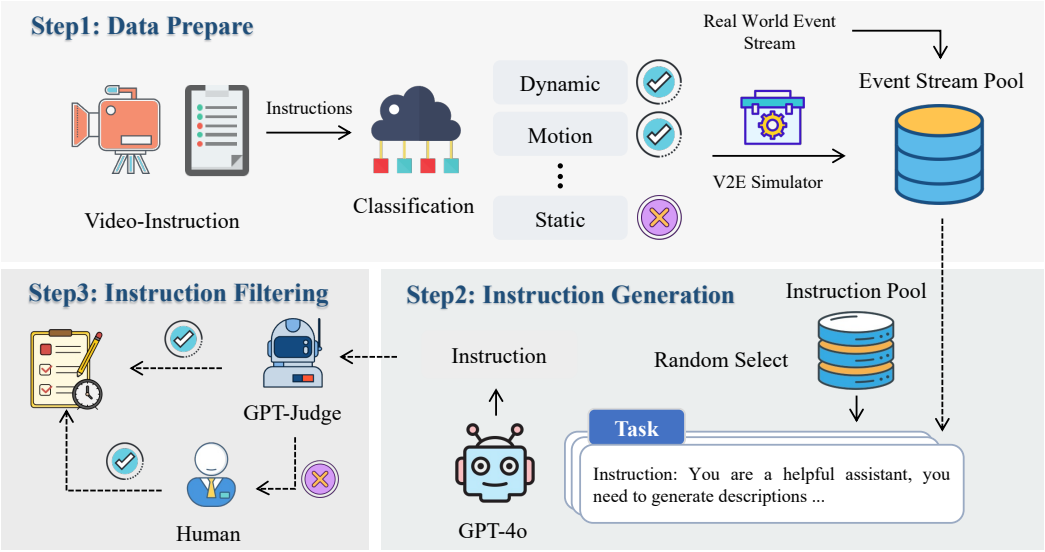


Figure 7: Overview of the instruction data construction pipeline for the EventMind dataset. The process includes data preparation with event simulation (Step 1), instruction generation via GPT-4o (Step 2), and quality filtering using GPT-Judge and human verification (Step 3).

(MLLMs) across captioning, temporal reasoning, instruction following, and fine-grained event stream understanding. We believe this standardized dataset will accelerate research on event-based MLLMs.

As illustrated in Fig. 7, our EventMind dataset is constructed via a multi-stage pipeline comprising motion classification, GPT-assisted instruction generation, and rigorous quality filtering. Table 6 provides an overview of the raw data sources and the task-specific distribution statistics. Fig. 8 showcases representative examples from EventMind, covering a range of tasks including fine-grained question answering, multiple-choice QA, scene captioning, and human action understanding.

## D Evaluation Tasks

**Simple Caption.** This task involves concise single-sentence descriptions of short event streams, primarily focusing on visual-language alignment. It is used in the first stage of curriculum learning to initialize event-text grounding. The dataset contains 200k instruction samples.

**Human Action QA.** This task centers on identifying and reasoning about specific human actions, covering over 700 distinct motion categories. It is designed to enhance the model's temporal reasoning and fine-grained action understanding. The dataset includes 30k annotated samples.

**Scene Caption.** This task provides detailed descriptions of event-rich scenes, emphasizing environmental context and background semantics. It improves the model's ability to generate coherent and complete global summaries. The dataset contains 90k instruction samples.

**MCQA (Multiple Choice QA).** This task presents structured multiple-choice questions, requiring the model to select the correct answer from given options. It primarily evaluates instruction-following and discriminative reasoning capabilities. The dataset includes 10k QA pairs.

**FGQA (Fine-Grained QA).** This task focuses on event-specific question answering at a fine-grained level, targeting subtle spatial or temporal details within a dynamic scene. It aims to improve the model's sensitivity to localized event cues. The dataset provides 60k examples.

**EventQA.** This task involves open-form questions grounded in temporally unfolding events, emphasizing understanding of causality, object interaction, and motion phases. It improves general event reasoning under natural language queries. The dataset includes 90k instances.

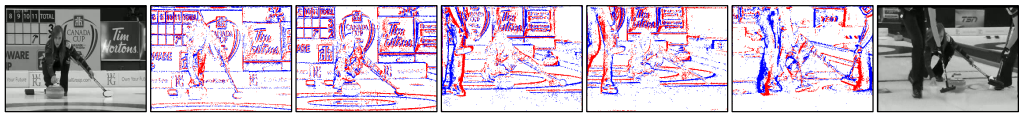

**Instruction:** Are there any noticeable changes in the player's brushing technique or direction while brushing the ice floor?

**FGQA**

**Answer:** No noticeable changes are in the person's brushing technique or direction.

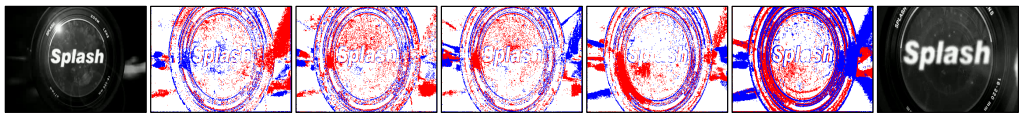


**Instruction:** What letter combination is prominently shown in the image sequence?

A. Flash B. Splash
C. Slash D. Crash

**MCQA**

**Answer:** (B) Splash

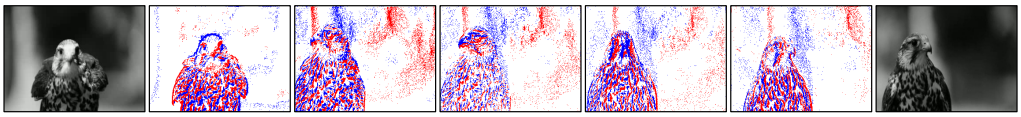

**Instruction:** What is happening in this scene?

**Scene Caption**

**Answer:** A bird is initially facing forward, then gradually turns its head to the side. The motion sequence captures the transition in head orientation, indicating a natural scanning or attention shift.

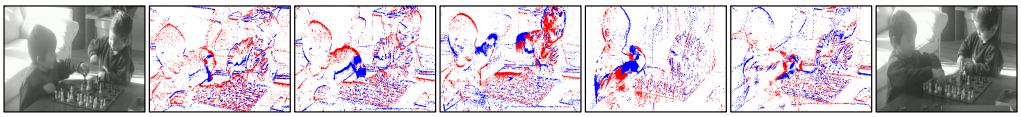

**Instruction:** What human action is depicted in this event stream? First, identify the action performed by the human, and start with 'It is + the name of the action. Please step by step.

**Human Action QA**

**Answer:** It is playing chess. The sequence shows two individuals seated across from each other at a table, with their hands moving pieces on a chessboard. One individual reaches out to move a piece, followed by the other responding with a counter-move…

Figure 8: An example from our EventMind dataset illustrating four typical tasks (i.e., fine-grained QA, multiple-choice QA, scene captioning, and human action QA).

**Motion Caption.** This task targets the generation of action-centric scene descriptions, with an emphasis on temporal ordering and motion dynamics. It enhances the model's ability to capture and narrate event transitions. The dataset includes 30k annotated captions.

## E Evaluation Metrics

We design four evaluation metrics to assess all models (GDC, FGQA, MCQA, and HAQA). Specifically, GDC measures the model's capability of scene description, while FGQA evaluates fine-grained

Table 7: Token-to-First-Token (TTFT) latency comparison across models under 5 bin and 1,000 bin temporal scales. Note that our EventFlash achieves the best overall performance, significantly improving latency while maintaining or exceeding accuracy.

| Model | Scale | EventEncoder | LLM Backbone | TTFT (s) | Average acc |
|---|---|---|---|---|---|
| 5 bin scale | | | | | |
| EventGPT | 7B | clip-vit-large-patch14-336px | Vicuna-v1.5 | 0.59 | 74.7 |
| EventFlash-Zero | 7B | clip-vit-large-patch14 | Qwen2.5 | 0.70 | 73.8 |
| **EventFlash(Our*)** | 7B | clip-vit-large-patch14 | Qwen2.5 | **0.32** | **76.8** |
| 1000 bin scale | | | | | |
| EventFlash-Zero | 7B | clip-vit-large-patch14 | Qwen2.5 | 2.97 | 62.2 |
| **EventFlash(Our*)** | 7B | clip-vit-large-patch14 | Qwen2.5 | **0.73** | **66.8** |

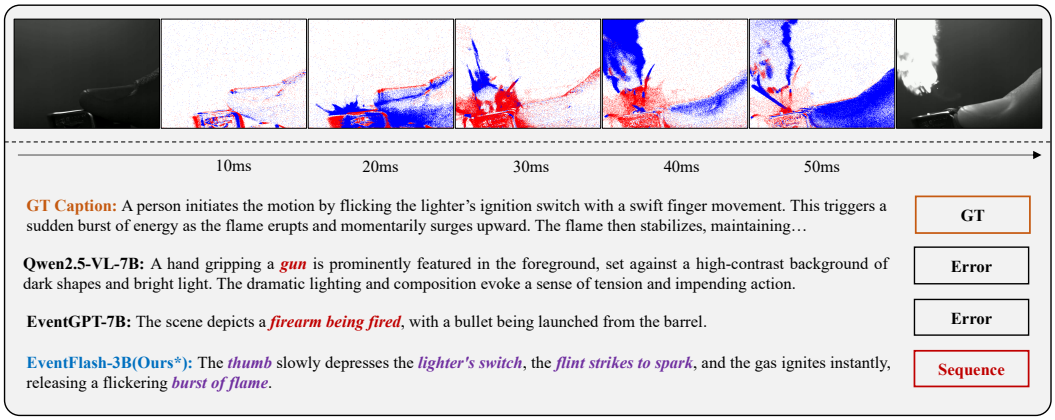


Figure 9: Representative visual comparison between EventFlash, EventGPT, and other open-source MLLMs, highlighting their performance under challenging high-speed motion scenarios.

scene question answering. Both are conducted in an open-set QA manner and assessed using GPT as a judge. To ensure a more objective evaluation, MCQA and HAQA are formulated as multiple-choice questions. As shown in the Table. 1, we conduct experiments on our constructed EventMind dataset as well as the EventChat-Sub dataset, which is derived from the publicly available EventGPT dataset, where we randomly sample 1,000 instances for evaluation.

**Global Detailed Captioning (GDC).** This metric evaluates the model's ability to generate rich scene-level descriptions. It emphasizes coverage, fluency, and relevance in captioning tasks.

**Fine-Grained Question Answering (FGQA).** This metric reflects the model's capacity to capture fine spatial and temporal details, measuring its precision in localized event reasoning.

**Human Action QA.** This metric assesses the model's understanding of human motion, especially its ability to distinguish between subtle action variations across time.

**Multiple Choice QA (MCQA).** This metric evaluates the model's instruction-following and decision-making capabilities through structured reasoning over candidate answers.

## F More Results

**Qualitative Analysis.** To better evaluate the performance of EventFlash, we select several challenging cases from the test set of EventMind and visualize the results in comparison with open-source state-of-the-art video-based MLLMs (e.g., Qwen2.5-VL) and event-based MLLMs (e.g., EventGPT), as shown in Fig. 9 and Fig. 10. The results show that EventFlash consistently outperforms other models in event-driven scenarios. Under high-speed motion conditions with a temporal span of only 50 ms,

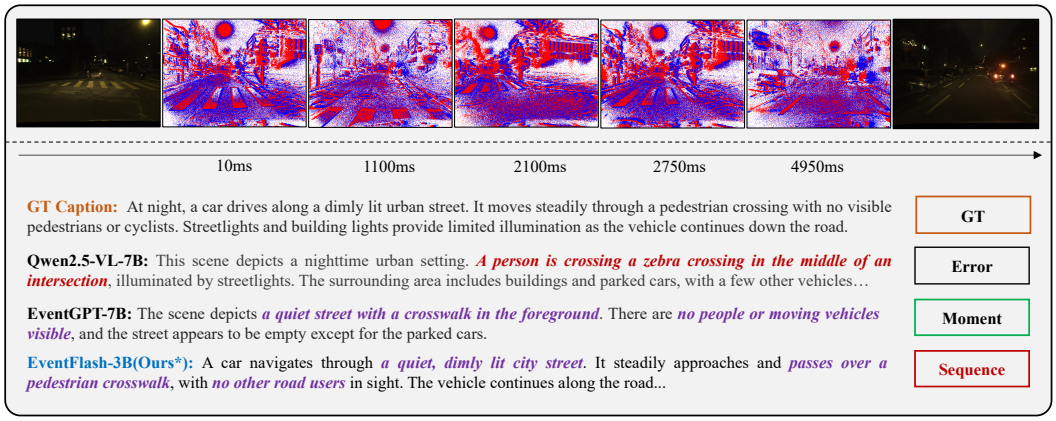


Figure 10: Representative visual examples from our EventMind dataset, comparing EventFlash, EventGPT, and other open-source MLLMs. Not that, our EventFlash achieves the best performance under challenging low-light scenarios.

EventFlash exhibits superior temporal sensitivity and more accurate scene understanding, highlighting its clear advantage in handling fine-grained, fast-evolving dynamic events. In low-light environments, EventFlash also maintains robust performance with accurate descriptions and reasoning, whereas EventGPT, although capable of capturing static scene elements, tends to provide only moment-level observations without modeling the full temporal dynamics of the scene.

**Efficiency Analysis.** Our comprehensive evaluation compares the inference efficiency of EventFlash against both EventFlash-Zero and EventGPT across two distinct temporal scales: 5-bin and 1,000-bin configurations. As depicted in Table 7, EventFlash demonstrates significant improvements in Time-to-First-Token (TTFT) latency across both experimental conditions. For the 5 bin setting, EventFlash reduces TTFT from EventGPT's 0.59s baseline to 0.32s, representing a 45.8% reduction in latency. For the challenging 1,000 bin configuration, our EventFlash achieves a dramatic 75.4% improvement over the baseline EventFlash-Zero, cutting latency from 2.97s down to 0.73s. These substantial gains in processing speed highlight how our novel sparsification strategy not only enhances immediate inference efficiency but also maintains robust scalability when handling longer temporal sequences. Importantly, these latency improvements are achieved without compromising model accuracy. In fact, EventFlash maintains comparable or superior performance metrics across all evaluated scenarios. The consistent performance advantages indicate that our EventFlash maintains efficiency across diverse real-world application requirements.

## G LLM USAGE

We only used LLMs for language polishing, while no LLMs were involved in the creative aspects or the development of the innovations in our paper.